

GT2011-45(%%)

**DEVELOPMENT OF AN OPTIMIZATION DESIGN METHOD FOR TURBOMACHINERY
BY INCORPORATING THE COOPERATIVE COEVOLUTION GENETIC ALGORITHM
AND ADAPTIVE APPROXIMATE MODEL**

Peng SONG; Jinju SUN^{*}; Ke WANG, Zhilong HE

School of Energy and Power Engineering, Xi'an Jiaotong Univ.,
28 West Xianning Road, Xi'an, China, 710049

ABSTRACT

An optimization design method is developed, which is motivated by the optimal design of a cryogenic liquid turbine (including an asymmetric volute, variable stager vane nozzles, shroud impeller and diffuser) for replacement of the Joule-Thomson throttling valve in the internal compression air-separation unit. The method involves mainly three elements: geometric parameterization, prediction of objective function, and mathematical optimization algorithm. Traditional parameterization approach is used for the geometry representation, while some novel work in the latter two aspects (i.e. objective function evaluation and optimization algorithm) is done to reduce the computing time and improve the optimization solution.

A modified Cooperative Coevolution Genetic Algorithms (CCGA) is developed by incorporating a modified variable classification algorithm and some new self-adapted GA operators, which help to enhance the global search ability with an excessive number of optimization variables. Design of Experiment (DOE) is carried out to initialize the kriging approximation model, which is used to approximate the time-costly objective function. Then the CCGA is started, and once a potential superior individual is found, a decision will be made by the in-house code on whether or not it needs a updating. If required, the true objective function prediction based on the real model will be conducted and the obtained value of objective function will be used to update the kriging model. In such a way, the CCGA can complete its optimal searching with a limited number of real evaluations for objective function. All the above features are integrated into the optimization framework and encoded for the optimal turbine design. In addition, CFD software ANSYS CFX is used for the real objective function evaluations, and a well-organized batch code is developed by the authors for calling the CFD simulation which helps to promote this automation of the optimization process.

For validation, the optimization method is used to solve some classical mathematical optimization problems and its effectiveness is demonstrated. The method is then used in the optimal design of the cryogenic liquid turbine stage, it is demonstrated that the optimal design method can help to reduce

significantly the searching time for the optimal design and improve the design solution to the liquid turbine.

1 INTRODUCTION

In many cryogenic processes, liquids are often expanded from high pressure to a lower pressure level. Traditionally the expansions are completed by using a Joule-Thomson (J-T) valve, which will not only waste considerable pressure-head and reduces largely the throttling process efficiency, unexpected temperature rise will also increase liquid losses and cavitation damage[1]. Alternatively, a cryogenic turbine can be used to replace the J-T valve [2]. With a smoothly pressure drop processing, the pressure head of liquefied gas was converted to electricity. The throttling process in the turbine is more isentropic in comparison with that in a J-T valve, and energy dissipation may be reduced to a minimum, a temperature rise in the cryogenic system can then be controlled. A replacement of J-T valve by cryogenic liquid turbine can produce considerable overall benefits in both air-separation unit and LNG (Liquefied Natural Gas) system. In an internal compression air-separation unit, a use of liquid turbine could reduce 3% of the total energy consumption [3]; in a LNG system, electricity of 500,000 dollars was saved annually through the replacement as reported in [4].

In previous work, a single stage cryogenic liquid turbine is designed for a large-scale internal compression air-separation unit to replace the Joule-Thomson valve and recover energy from the liquefied air during throttling process [5][6]. It includes an asymmetric volute, variable stager vane nozzles, impeller and diffuser. The turbine stage flow and performance is simulated by CFD, and the predicted overall efficiency at the design condition is about 84.83%, clearly there exist some potentials for improvement. An optimization design method is developed in the present study, which is motivated by the optimal design of the cryogenic liquid turbine.

To achieve further overall performance gain, a novel optimization design method is developed to optimize the turbine geometry in a stage environment, and validated in the present study.

It is demonstrated by our previous work that turbine performance and flow are sensitive to the impeller geometric

^{*} Contact author: Dr Jinju SUN, jjsun@mail.xjtu.edu.cn

parameters, nozzle vane stagger angle and geometry, and radial gaps between the impeller and nozzle [5]. To allow for the influence of all these geometric parameters, the turbine stage must be optimized in a real stage environment with CFD simulation for predicting the stage overall performance. Clearly such as an optimization problem involves a number of variables and considerable CFD simulations and it can be much time consuming. Thus, how to reduce the optimal searching time and obtain a relatively global solution is the major concern in the present study of the optimization design method development, and some efficient optimization methods or algorithms must be incorporated in the turbine design optimization method.

In recent years, stochastic optimization methods, such as Genetic algorithms (GA) and Evolution strategies (ES) are used more widely in the optimization of turbomachinery. All these population-based search algorithms help to find the global solutions, but have also inherent drawbacks, in particular, the convergence speed is much slow and considerable time-consuming CFD computation are often required for candidate solutions. Some work has been done by the previous investigators to improve the conventional GA algorithms and the better globality and convergence speed are achieved [7][8].

For the purpose of optimization time reduction, some surrogate models are incorporated into the design optimization. Applications of Artificial Neural Networks (ANN) in the nonlinear aerodynamics optimization are reported in [9]. Ref. [10] reviews the global optimization approaches for aerodynamics and propulsion components, which rely on the response surface methodologies (RSM). Ref. [11] presents the implementation of kriging approaches with the standard GA. However, with these methods, once the approximation model is set up, it will be used through the entire optimization process without any updated modifications; clearly such a feature largely influences the prediction accuracy of objective function restrains effectiveness of the optimal searching. A modified method is developed and presented in [12], where the surrogate model is updated accordingly as the optimization proceeds, which has helped to reduce the computation cost and produce more accurate prediction, but it is only used for the simple mathematical problem test, whether it is suited for the complicated geometry optimization, such as turbomachinery design optimization, hasn't yet been justified.

In the present study, an improved optimization-procedure is proposed, based on which an optimization method suited for turbomachinery design is developed. The method involves mainly three elements: geometric parameterization, prediction of objective function, and mathematical optimization algorithms. Traditional parameterization approach is used for the geometry representation, and some novel work is done in the latter two aspects. An improved CCGA is proposed and the auto-updated approximate model is incorporated, which is updated with the optimal searching process by calling CFD simulations. Both have helped to reduce the computing time and improve the optimization solution in the optimization of the liquid turbine in a real stage environment.

2. NUMERICAL METHOD FOR FLOW AND PERFORMANCE PREDICTION

In the optimization problem, performance must be predicted at each or several searching steps, based on which the optimal searching direction for the successive steps can be determined, in such a way, the optimal solution is finally obtained.

In the present study, the CFD method is used for predicting flow and performance prediction of the turbine, and ANSYS CFX is used. To validate the CFD method, flow simulation is conducted firstly for the original liquid turbine at design condition, and a brief description of the method is given below together with the obtained numerical results.

2.1 Physical Model and Grid Generation

To achieve an accurate prediction of turbine performance, flow simulation is conducted in a real entire stage environment. The physical model for simulation consists of the asymmetric volute, variable stager vane nozzles, shroud impeller (no tip clearance is considered) and diffuser, and shown in Figure 1

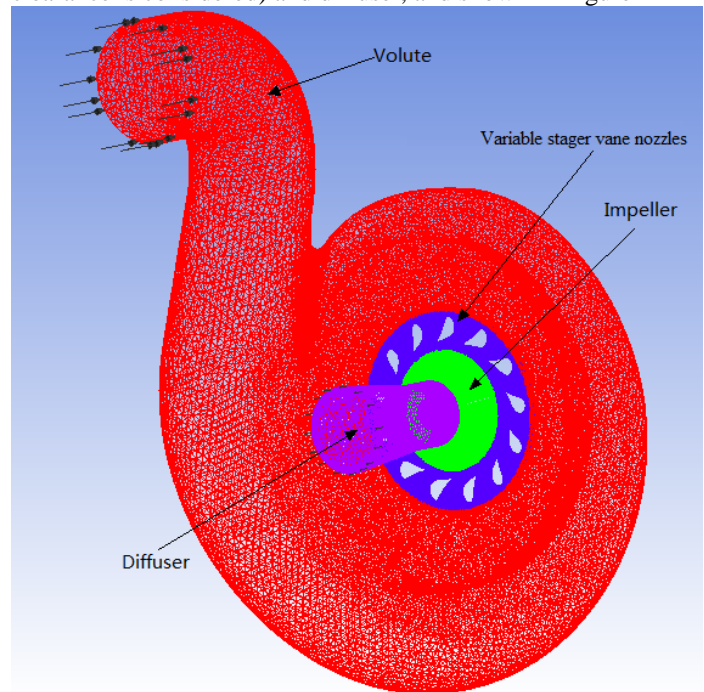


Fig. 1 Physical model for stage and total grid

ANSYS-ICEM is used to generate the unstructured mesh with tetra elements to define the volute and diffuser zone and prism cells to refine near wall mesh. The structured multi-block grids are generated by the CFX-Turbogrid with an H/J/C/L and J grid topology for nozzle vane and shroud impeller.

Grid for original geometry turbine

Grid generated for the original turbine geometry. The overall mesh size of original design for the entire computational domain is 1894667, where 661817 are for the volute, 579150 for the nozzles, 550800 for impeller, and 102900 for diffuser respectively. Figure 2 presents the grid generated for the nozzles and impeller.

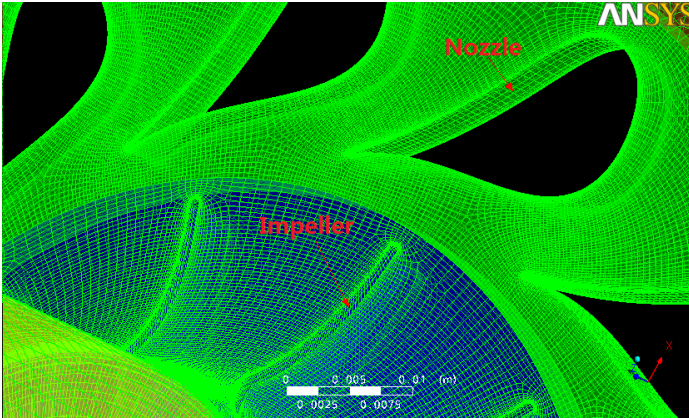


Fig. 2 Grid of nozzle and impeller

To validate the grid dependency, a large grid size of 2.5 million is used in flow simulation (meshes in the near wall regions are mainly refined, such as end wall, and leading and trailing edge of the nozzle and impeller blades). The calculation time for convergence increases about 30%, but it doesn't produce visible difference in numerical results; thus a moderate grid size of 1894667 is used throughout the present study.

Automated grid generation for optimization process

In the present study, the nozzle and impeller geometry is optimized simultaneously, and geometry of both will be varied, thus grid for CFD simulation should be generated accordingly for the updated geometry of both nozzle and impeller. Clearly grid automation is essential for the CFD prediction callings in the optimization process. The new feature of TUBOGRID in the ANSYS can satisfy this requirement and it is used in the present study, namely the ATM optimized topology, which is an alternative to the standard topologies, this topology type enables us to create high-quality meshes with minimal effort; there is no need for control point adjustment[13]. With this new feature, grids of the updated nozzle and blade geometry are generated automatically. In addition, the grids are also refined at the near wall regions, such as end wall, and leading (LE) and trailing edge (TE) of the nozzle vane and impeller blade. All have been done automatically. The established grid files are then imported to ICEM-CFD, the minimum face angel and maximum aspect ratio of the grids will be checked sequentially to insure a good grid quality for CFD calculations; and the grids of single flow channel are duplicated to circumference as a whole grid, only which can be used in flow simulations.

2.2 Numerical Simulation of the Turbine Stage

CFD simulation was carried out in a stage environment using commercial software ANSYS-CFX. The solver of ANSYS-CFX utilizes a control volume method based on finite volume discretization scheme to solve the Navier-Stokes equations in their conservation form with so-called coupled algebraic multigrid technology.

The steady flow models are used in the present study and $k - \epsilon$ turbulence model is adopted. When setting for simulations of liquid pumps and turbines, the $k - \epsilon$ and Shear Stress Transport models are appropriate choices for modeling

turbulence. Within CFX, the $k - \epsilon$ turbulence model uses the scalable wall-function approach to improve robustness and accuracy when the near-wall mesh is very fine. The scalable wall functions allow solution on arbitrarily fine near wall grids, which is a significant improvement over standard wall functions [13].

Frozen rotor model is used at the interface of nozzle-impeller and impeller-diffuser. This model produces a steady state solution to the multiple frame of reference problems, with some account of the interaction between the two frames. The frozen rotor model has the advantages of being robust and using less computer resources than other frame change models [13].

In particular, the thermal physical property of liquefied air redefined by NIST's (National Institute of Standards and Technology) software EREFPROP is incorporated into CFX solver, which permits the solver be able to deal with the liquefied air as compressible flow in the present study.

Total pressure and total temperature are imposed at the volute inlet boundary, while static pressure is specified at outlet. No-slip and adiabatic conditions are applied to solid surfaces of the blade, hub and shroud, and outlet.

One of the most important features of ANSYS CFX is its use of a coupled solver, in which all the hydrodynamic equations are solved as a single system. The coupled solver is faster than the traditional segregated solver and fewer iterations (less than 200 iterations generally) are required to obtain a converged flow solution [13]. The most important factor for convergence is timescale. To justify the best setting, different timescale factor including 1, 5, 10 and 20 are set to the CFX-solver. Finally, the timescale factor shows a stable and quick convergence.

The simulation runs on a workstation of 2 2.93GHz×8 Xeon CPUs and 32GB RAM and it converges within the max iterations (set to be 300), and the running time is about 110 minutes. The table 1(a) presents the obtained overall turbine performance and some typical flow parameters for the nozzle and impeller, and variation of flow parameter in each component is visible. The predicted overall isentropic efficiency is 84.83 %, and power output is about 187.93kW.

To test the influence of different boundary conditions, the flow rate is specified at turbine outlet rather than the static pressure. The simulation has converged after about 300 iterations, and the obtained flow parameters and overall performance are compared with that of the static pressure outlet condition, and both agree well, as shown in table 1.

Table 1 Flow parameters and overall performance predicted using different outlet conditions

(a) Static pressure outlet

Volute inlet pressure	MPa	7.27
Volute inlet temperature	K	96.98
Impeller inlet static pressure	Mpa	3.96
Impeller inlet absolute velocity	m/s	87.26
Impeller inlet relative velocity	m/s	28.84
Impeller outlet absolute velocity	m/s	33.62
Diffuser outlet relative velocity	m/s	33.41
Diffuser outlet static pressure	Pa	0.58

Mass flow rate	kg/s	26.07
Power output	kW	187.64
Isentropic efficiency	%	84.70

(b) Massflow rate outlet

Volute inlet pressure	MPa	7.27
Volute inlet temperature	K	96.98
Impeller inlet static pressure	Mpa	3.95
Impeller inlet absolute velocity	m/s	88.38
Impeller inlet relative velocity	m/s	29.87
Impeller outlet absolute velocity	m/s	33.81
Diffuser outlet relative velocity	m/s	33.50
Diffuser outlet static pressure	Pa	0.58
Mass flow rate	kg/s	26.07
Power output	kW	187.93
Isentropic efficiency	%	84.83

In the optimization procedures, the design flow rate is specified, and the turbine performance (i.e. overall expansion ratio and efficiency) are optimized for this design flow rate.

3 DESIGN VARIABLES AND OBJECTIVE FUNCTION

In the optimization design problems, it is very important to identify the design variables and establish the objective functions of optimization. For shape design, design variable must be obtained on basis of shape parameterization. In turbomachinery optimization, the overall performance is commonly chosen as the objective function. However, it is noted the overall expansion ratio and efficiency often changes reversely with a variation in the shape geometry, thus a good compromise between the two performance parameters should be considered properly when establishing the objective function. Both issues are discussed brief below for the specified liquid turbine.

3.1 Design Variables and Geometric Representation

The 2-dimension nozzle vane is parameterized using two cubic B-spline curves, where 8 control points are used (coordinates of the leading and trailing edges, point 1, and point 8 are fixed), as shown in Figure 3. The upper and lower surfaces of vane are fitted respectively. To reduce the number of optimization variables and subsequent optimization convergence time, ordinates of point 2, 3, 4, 5, 6 and 7 are also held unchanged. Thus there are only 6 variables used to represent the nozzle vane shape.

Clearly the above treatment can compromise the optimized results, and such a consideration is only for the purpose of simplification and fast solutions. All these constraints may be eliminated in the future study to achieve a larger performance gains.

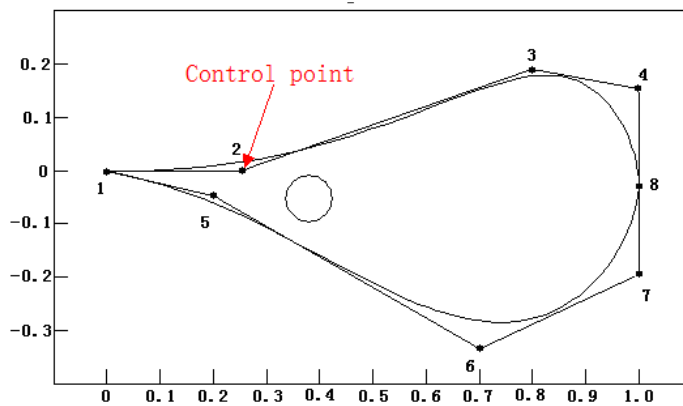


Fig. 3 Representation of Nozzle

In addition, the turbine is designed with variable nozzle vane staggers, as shown in Fig.4, and it is demonstrated from our previous investigations reported in [5], that the turbine flow and performance is sensitive to the nozzle vane stagger angles, to consider such effect, the stagger vane angle is included as one additional variable.

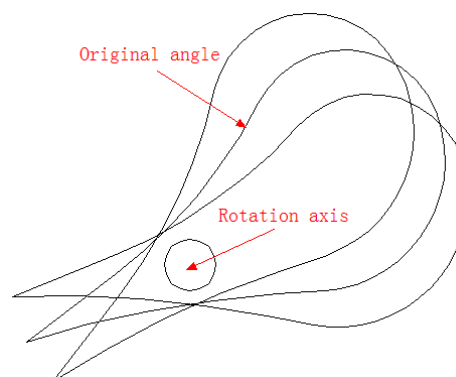
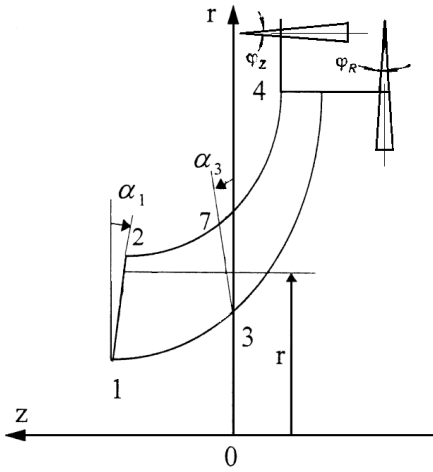


Fig. 4 Variable stagger vane of nozzle

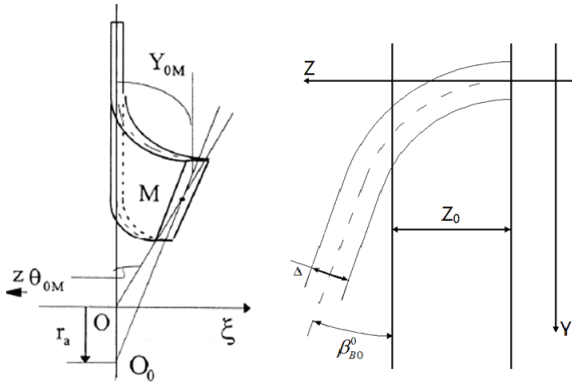
Parameterization of the impeller blade shape is essential during optimization process, which must be conducted according to the geometric characteristics. The turbine impeller geometry is a combination of the work wheel and inducer. The impeller meridional profile is represented by an elliptic-curve equation, Fig.5 (a), while the inducer is sort of the cylindrical-parabola surface, Fig.5 (b). Based on the above mentioned geometric features, the analytical method is chosen to parameterize the impeller.

For purpose of simplicity, some geometric parameters remain unchanged, and five parameters are chosen as the design variables, $\alpha_1, \alpha_3, \beta_{B0}^0, \varphi_R$, and φ_Z , and shown in the following figures. Where φ_R represents the angle between pressure surface and suction surface of the impeller blade in the radial direction; φ_Z the angle between pressure surface and suction surface of the impeller blade in the axial direction; α_1 the angle between the external end-face of inducer and radial direction; α_3 the angle between the internal

end-face of inducer and radial direction; and β_{B0}^0 the blade angle in the average-radial of external end-face of inducer;



(a) Impeller meridional profile



(b) $R-\theta$ Projection (c) Cylindrical section expansion

Fig. 5 Parameterization of impeller

In the optimization of turbine stage, it is supposed that the nozzle vane geometry and stagger, and impeller geometry vary simultaneously. As mentioned in the above analysis, 7 variables are used for the nozzle representation and 5 variables for the impeller, thus total number of variables used in the liquid turbine optimization is 12.

3.2 Objective Function

Definition

For the optimization problem, it is important to define a suited objective function. For the present turbine design, a high-level of overall efficiency is expected together with a prescribed expansion ratio when holding the flow rate. Thus a good compromise between efficiency and expansion ratio is required during optimization. A combined objective function is established based on a linear combination of the overall efficiency and expansion ratio, and written as

$$obj(x) = C_1(1 - eff) + C_2 \left(1 - \frac{Pr}{Pr^0} \right)$$

Where Pr denotes the expansion ratio, Pr^0 the value of Pr for original turbine geometry, eff the efficiency. C_1 and C_2 are the empirical coefficients and evaluated according to the variation range of Pr and eff .

During the optimization procedure, 120 CFD experiments are carried out to initialize the kriging model. The variation range of Pr and eff is obtained by the statistics of the initialization experiment data, and then C_1/C_2 calculated through the following expression:

$$\frac{C_1}{C_2} = \frac{\max \left[1 - \frac{Pr}{Pr^0} \right] - \min \left[1 - \frac{Pr}{Pr^0} \right]}{\max [1 - eff] - \min [1 - eff]}$$

In the present study, C_1 and C_2 take the value of 4 and 0.03 respectively. And both are calculated from initialization CFD experiments and held in the entire optimization process.

Automatic evaluation

In the present optimization process, the objective function is evaluated automatically and updated at each or over several steps by calling the CFD simulations. Fig.6 presents the flow chart showing the procedure for establishing the objective function. The entire process of CFD calling, ranging from the geometry construction of the modified nozzle and impeller to establishment of the objective function, is realized automatically through an inhouse batch processing code, which is developed based on the batch model proposed by the authors.

To further illustrate how the objective function is evaluated automatically, the procedure is described herein by reference to Fig.6. Once required by the optimization process through the batch code calling, the geometry generation function will be enabled to parameterize the modified nozzle blade and impeller shape. In the second step, the parameterized geometry is imported to CFX-TurboGrid and meshed automatically by the ATM topology. In the third step, setting up of the simulation is completed, including the boundary conditions, physical properties, turbulence model and convergence accuracy. In the next step, the CFX-solver is started by the batch code and runs with local parallelization. As the simulation has converged, a circumferential average procedure will be carried out on the inlet and outlet of the stage, some flow information such as averaged static pressure, averaged temperature, axis torque will be obtained by circumferential integral average; the thermal physical property can be obtained by calling from NIST's software REFPROP; then the isentropic efficiency and expansion ratio are calculated, based on which, the objective function can be then established by using the definition equation given in section 3.2.

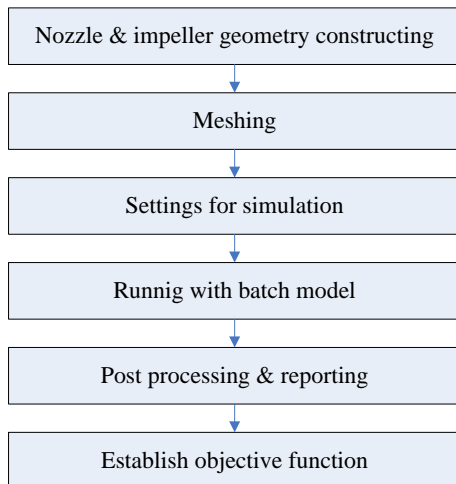


Fig. 6 Flow chart of complete CFD calling

4 OPTIMIZATION FRAMEWORK

In the present study, an optimization design method is developed, which is motivated by the optimal design of stage cryogenic liquid turbine. The method involves mainly four elements: geometric parameterization, automatic calling of CFD simulations, prediction of objective function, and mathematical optimization algorithms. As described the section 3, the traditional parameterization methods are used for representing the impeller and nozzle geometry; the linearly combined objective function is established for the overall efficiency and expansion ratio, and updated automatically by calling of CFD simulations during the optimal process. Some novel work is conducted for improving the mathematical optimization algorithm and method to reduce the searching time for the optimal solutions, as is detailed in section 5.

The developed methodology for blade optimization is incorporated into a computer program, and Fig.7 presents the corresponding flow chart. As illustrated in the figure, it involves mainly five modules: Geometry parameterization, kriging model initialization, Classification of variables, CCGA and self-updating of kriging model. Main function of each module is briefly described below.

Geometric parameterization: the nozzle blade and impeller shape geometry is parameterized by calling the inhouse geometry parameterization code, and it is developed based on the analytical method for impeller and cubic B-spline approach for nozzle blades, as described in section 3.

Kriging model initialization: The kriging model is initialized by the DOE (Design of Experiment) method based on 120 numerical samples, which is obtained though the CFD simulation of the turbine flow in a real stage environment. It is used to predict the turbine performance for every new design as an approximation for the CFD result, and clearly such a replacement of time-consuming CFD simulation can help to reduce the computation time.

Classification of variables: In this module, the conventional GA incorporated with the initialized kriging model runs for some steps to obtain sufficient statistical data. Based on the statistical analysis of the obtained numerical results, relevance

between any two design variables is then quantified, based on which the design variables are classified.

CCGA: CCGA decomposes a high-dimension problem into some sub-problems and uses evolutionary algorithm to solve them gradually, in such a way, the original high-dimension problem will be solved. At first step, the original problem is decomposed into n sub-problems by the variable classification algorithm, and each of which is handled by one species. Each species involves a part of the variables. Then genetic operators will be applied to all the species, each can evolve independently like normal GAs. Only when an individual in one species is evaluated, it will be combined with other individuals from the other species, and the fitness of the resulting chromosome is evaluated and returned. When termination condition is achieved, the CCGA will converge at a global optimum design together with all the species. In the present study, some improvements have been made on the CCGA by the authors to ensure the CCGA searching converge at a global optimum design with less searching time.

Automatically updated kriging model: In the CCGA procedure, once a potential superior individual is found on the basis of statistics, a decision is made by the in-house code on whether or not the CFD simulation should be called for performance (i.e. the fitness or objective function) prediction of the new design geometry. If the fitness is obtained based on CFD simulation rather than the approximated model, it will be termed ‘true fitness’ in the following context and will be saved in the database to update the kriging model. As a result, with less calling of CFD simulations, accuracy of the kriging model used in the present study can be sustained.

In addition, the entire automatic procedure involves several elements: the blade generation, CFD simulation calling and setting-up, approximation model and optimization algorithms. All the elements are incorporated into C++ codes and intergraded into an automatic optimization framework.

Convergence checking: In the CFD based optimization problem, the convergence check of each CFD solution is one of the most crucial and difficult steps. To do this, the authors have developed an in-house C++ code, which compares the flow parameter values obtained from the successive iterations and then justify whether the simulation is converged or not.

The maximum number of iterations is firstly assigned, once the maximum has been reached, and then the in-house C++ code will check the residual of flow parameters, such as pressure, temperature, velocity and overall flow rate. If the residual is larger than the prescribed value (i.e. 10^{-4}), then the maximum number of iterations will be increased, and iterations of flow simulation will be continued until the residual criterion is satisfied.

In addition, the entire automatic procedure involves several elements: the blade generation, CFD simulation calling and setting-up, approximation model and optimization algorithms. All the elements are incorporated into C++ codes and intergraded into an automatic optimization framework.

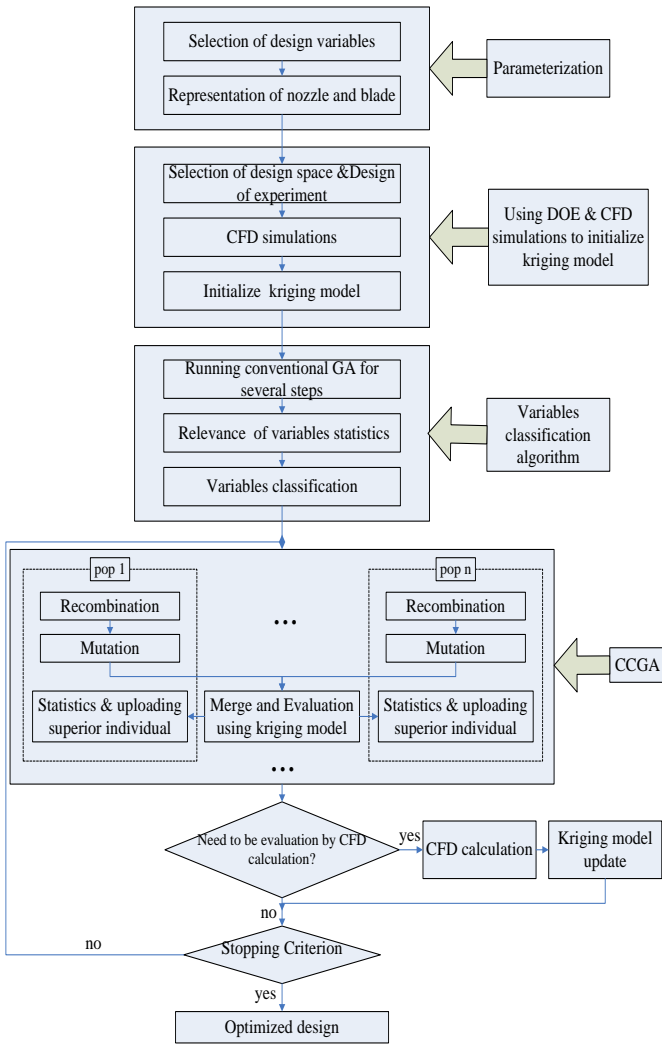


Fig.7 Flowchart of Optimization Framework

5 OPTIMIZATION ALGORITHM AND METHOD

As mentioned above, the optimization design method is developed for the optimal design of stage cryogenic liquid turbine, and involves mainly four elements: geometric parameterization, automatic calling of CFD simulations, prediction of objective function and mathematical optimization algorithms. In this section, the optimization algorithm and method as used in the present study are described and some improvement done by the authors highlighted.

In recent years, Genetic algorithms (GAs) and other evolutionary algorithms have been found of wide applications and become one of the most popular techniques for turbomachinery optimization. The reason for this is that GAs have some advantages over other methods, for example, the only information they need is the value of objective function, and they can also easily avoid getting stuck in local optima.

Figure 8 shows the principle of the basic Genetic algorithms, which mainly consists of recombination, mutation, selection and stopping criterion.

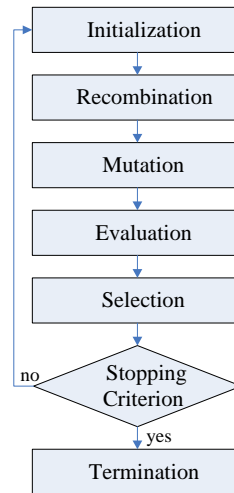


Fig. 8 Flowchart of Conventional GA

The conventional single-population GAs, however, have some inherent drawbacks: they commonly require considerable evaluations of the objective function with large scale CFD simulations, and often converge slowly, etc. For the large design space problems (e.g. turbomachinery optimization design), these drawbacks become much more severe, and clearly some modifications are required.

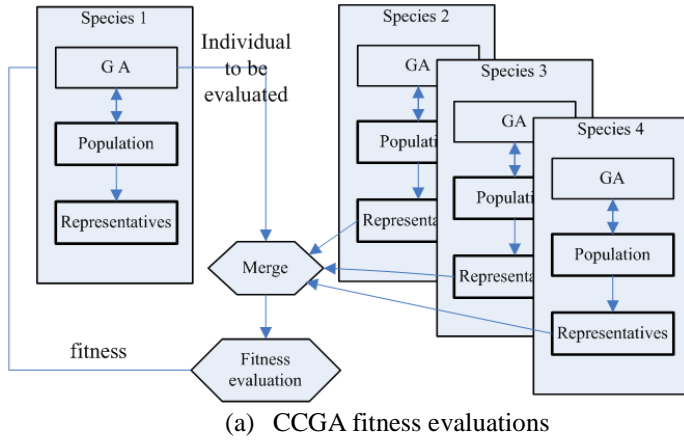
The Cooperative Coevolution Genetic Algorithm was proposed by Dejong and Potter to improve the conventional GAs, and initially designed for the optimization of mathematical functions [14]. Then it has been applied in the general architecture and some other areas, and attracted more and more research interests, for it is an effective approach to decompose complex problems into the sub-ones and achieve better performance.

In present study, the basic CCGA is modified by incorporating variable classification algorithm and self-adapted GA operators, while the automatically updated kriging model is integrated in the modified CCGA as objective function. They are incorporated into an optimization frame work code and used in the turbine optimization.

5.1 Cooperative Coevolution Genetic Algorithm

Complex optimization system problems can often be decomposed into several sub-problems, while all the sub-problems will interact with each other, and those are called co-evolution systems. Then complex problem can be solved through solving the subsystem problems and simultaneously allowing for the interactions between the relevant subsystem problems.

As shown in Figure 9 (a), the CCGA can decompose a large problem into some sub-problems and use evolutionary algorithms to solve them gradually so as to deal with the large problem. Clearly the fitness evaluation of CCGA is quite different from the conventional GA's. In CCGA, each species evolves respectively; and only when an individual needs to be evaluated, it will be merged with one or more representatives of other species. All the representatives constitute a sharing pool, when the evolution has converged, the sharing pool will also converge at the best individuals.



```

Decompose the problem into n species;
gen=0
for each species s
{
    randomly initialized population  $Pop_s(gen)$ 
    evaluate fitness of each individual in  $Pop_s(gen)$ 
}
while( termination condition=false)
{
    gen ++
    for each species s
    {
        select  $Pop_s(gen)$  from  $Pop_s(gen-1)$  based on fitness
        apply genetic operators to  $Pop_s(gen)$ 
        evaluate fitness of each individual in  $Pop_s(gen)$ 
    }
}

```

(b) main process of CCGA
Fig. 9 CCGA

Figure 9(b) shows the algorithm of CCGA. As the first step, the original problem is decomposed into n sub-problems, and each of which is handled by one species ($Pop_s(gen)$). Each species involves a part of the variables. After initialization, genetic operators will be applied to all the species and they evolve independently in the same way as the normal GAs. Once an individual in one species is evaluated, it will be combined with other individuals from the other species (i.e. the representatives sharing pool), and the fitness of the resulting chromosome will be evaluated and returned. As termination condition is achieved, the CCGA will converge at a global optimum design together with all the species.

Difficulties are often encountered in the applications of the conventional CCGA, since it is difficult to classify the variables. Without an appropriate variable classification, the algorithm can lead to a useless searching and mal solution. Thus, the present

study focuses on the variable classification and some improvement are made as described below.

Variable classification algorithm

In CCGA, the procedure of variable decomposition is one of the major issues. Wrong variables decomposition will lead to a useless searching and mal solution. Holland [15] indicates that crossover induces a linkage phenomenon. It has been shown that the CCGA works well only if the building blocks are tightly linked on the chromosome.

In the present study, to deal with the linkage-learning problem, a variables decomposition algorithm based on linkage identification is used [16].

The conventional GA runs t generations first, and statistics analysis is done for the existing population of GA. Then the relevance of two variables ($\rho(x_i, x_j)$) can be calculated, which will be used for variable classification.

Consider this n -dimension optimization problem:

$$\min f(x), x = (x_1, x_2, \dots, x_n)^T \in S \subset R^n \quad (1)$$

The population of GA in t generation can be written as the N_i vectors (each vector represents a individual)

$$X_i(t) = (x_{i1}(t), x_{i2}(t), \dots, x_{in}(t)), i = 1, 2, \dots, N_i \quad (2)$$

In this variable decomposition algorithm, the relevance of two variables $\rho(x_i, x_j)$ is calculated by:

$$\overline{X_{*i}}(t) = \frac{1}{N_i} \sum_{p=1}^{N_i} x_{pi}(t) \quad (3)$$

$$\sigma(x_{*i}(t)) = \sqrt{\frac{1}{N_i - 1} \sum_{p=1}^{N_i} (x_{pi}(t) - \overline{X_{*i}}(t))^2} \quad (4)$$

$$\rho(x_i, x_j) = \frac{1}{N_i} \cdot \frac{\sum_{p=1}^{N_i} (x_{pi}(t) - \overline{X_{*i}}(t))(x_{pj}(t) - \overline{X_{*j}}(t))}{\sigma(x_{*i}(t))\sigma(x_{*j}(t))} \quad (5)$$

The value of $\rho(x_i, x_j)$ represents the relevance of two variables. If two variables are highly relevant, they should not be separated and placed in the different groups.

Thus, a quick cluster analysis is applied based on the relevance of two variables to produce a good variable grouping through the recursive classification.

5.2 Improvements of CCGA

Some adaptive strategies including the simulated annealing are introduced into CCGA to promote the optimization convergence speed and solution globality. The classical evolutionary operators are replaced by the appropriately defined new operators.

Recombination(crossover)

In the conventional GA, search region is limited by initial populations, and the optimal is easily missed. An operator,

namely the simulative-binary recombination operator, is used to help the children to jump out of the limitative range of their parent's, and given by

$$\bar{x}_i^{child1} = 0.5 \left((1 + \beta) \bar{x}_i^{parent1} + (1 - \beta) \bar{x}_i^{parent2} \right) \quad (6)$$

$$\bar{x}_i^{child2} = 0.5 \left((1 - \beta) \bar{x}_i^{parent1} + (1 + \beta) \bar{x}_i^{parent2} \right) \quad (7)$$

Where \bar{x}_i^{child1} , and \bar{x}_i^{child2} are generated by $\bar{x}_i^{parent1}$ and $\bar{x}_i^{parent2}$ selected in the parents population. The value of β is determined by the random number of r in a scope of 0 ~1.

$$\beta = \begin{cases} (2r)^{1/(1+\eta)} & r \leq 0.5 \\ [1/(2-2r)]^{1/(1+\eta)} & r > 0.5 \end{cases}, r = \text{random}(0,1), \eta \approx 0.1 \quad (8)$$

Mutation

The improved mutation operators are used to adjust the amplitude of mutation automatically as the number of evolution increases.

$$x_k^* = \begin{cases} x_k + \Delta(t, b_k - x_k) & r \leq 0.5 \\ x_k - \Delta(t, x_k - a_k) & r > 0.5 \end{cases} \quad (9)$$

$$\Delta(t, y) = y \left(1 - r^{\left(1 - \frac{t}{T}\right)\beta} \right) \quad (10)$$

Where x_k^* is the modified x_k after mutation, t the number of evolution, and T the prescribed maximum number of evolution. The range of mutation is defined as $\Delta(t, b_k - x_k)$, and it takes the largest value at the beginning and then will decrease as the number of evolution increases.

Self-adaption strategy

The crossover rate (p_c) and mutation rate (p_m) are both self-adapted, which are controlled by the parameter t/T and the statistical results of a population (including the maxima, minima and averaged value of fitness), to avoid premature and improve globality of optimal solutions.

$$p_c = \begin{cases} \eta_1 \frac{f_{\max} - f'}{f_{\max} - f_{avg}} - \mu_1 \frac{t}{T} & f' \geq f_{avg} \\ \eta_1 - \mu_1 \frac{t}{T} & f' < f_{avg} \end{cases} \quad (11)$$

$$p_m = \begin{cases} \eta_2 \frac{f_{\max} - f}{f_{\max} - f_{avg}} + \mu_2 \frac{t}{T} & f \geq f_{avg} \\ \eta_2 + \mu_2 \frac{t}{T} & f < f_{avg} \end{cases} \quad (12)$$

Fitness self-adaptation

Fitness self-adaptation is derived from simulated annealing algorithm and used to shrink and/or enlarge the fitness difference for different individuals, and protect the better individuals and eliminate the worse ones.

$$f' = \exp \left(\frac{f}{\left(\frac{t-1}{1-e^{T+1}} \right) f_{\max}} \right) \quad (13)$$

5.3 Test on the improved CCGA

For the purpose of validation, the modified CCGA is tested by a bump problem with a well-known solution, and it is much smooth but contains many peaks, thus it is very hard to deal with for the most other optimizers. The problem is expressed below

$$\max f_1(x) = 10000 - 418.9829 \cdot N + \sum_{i=1}^{N_d} x_i \sin \left(\sqrt{|x_i|} \right) \\ , x_i \in [-500, 500], i = 1, 2, \dots, N \quad (14)$$

The maximum of this problem is 10000 and located at $x = (-420.9687, -420.9687, \dots)$.

Figure 10 shows the plot of the 2-D bump problem ($N = 2$).

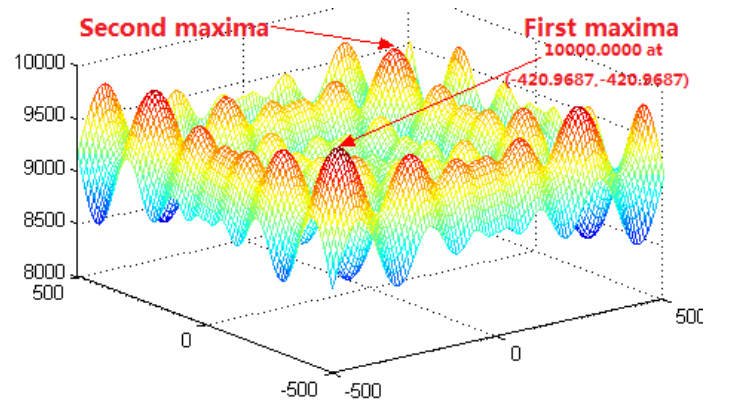


Fig. 10 Plot of 2-D bump problem

Three cases, $N=6$, $N=12$ and $N=20$, are used in the test and the above bump problem is solved respective for each case by the improved CCGA. To reduce the influence of randomness, each case has run 10 times. The converged generations of the CCGA for $N=6$, $N=12$ and $N=20$, are respectively 860, 1820 and 3200.

To illustrate the convergence of improved CCGA, the optimal path for the 12-dimension bump problem (i.e. N=12) is presented in Fig.11. Clearly it has converged after 1820 generations to the maxima, 10000.

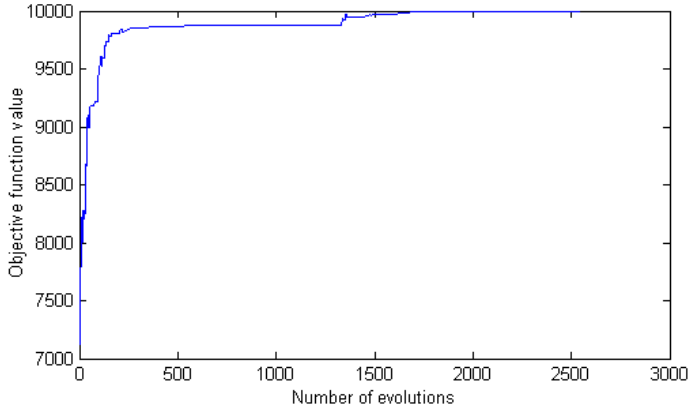


Fig. 11 Converge history of improved CCGA

5.4 Kriging Approximation Model

Another well-known drawback of GAs is the requirement of intensive CFD calling for evaluating the fitness (objective function), which is much costly in both computing time and resources aspects. In the present study, some surrogate models are established as an approximation to the real CFD prediction, which involving the response surface modeling, kriging models and artificial neural networks. These surrogate models are established by using limited number of real CFD experiments and predict the fitness (objective function) approximately, which can be used as a replacement of certain real CFD simulations.

Kriging model

In applications of the approximation models, the polynomial modeling is often one of the choices, which is created by performing a least square fit for a set of data. The polynomial modeling methods are initially developed to produce smooth approximation models of response data contaminated with random error found in typical physical (stochastic) experiments. Clearly it is improper to use these approximation models to a determinate experiment where there is no random error [17].

On the other hand, kriging interpolation functions, originally developed in the fields of spatial statistics and geostatistics, can easily capture the oscillatory response trends and have been shown to provide better fitting in multi-dimensional domains [18].

Kriging model utilizes the correlation between neighboring points to determine the overall function at an arbitrary point. In the kriging metamodels, the unknown function to be modeled is typically expressed as

$$\hat{y}(\bar{x}) = F(\beta, \bar{x}) + Z(\bar{x}) \quad (15)$$

Where \bar{x} is the vector variables, $F(\beta, \bar{x})$ is a regression model of \bar{x} with parameter β

$$F(\beta, \bar{x}) = \sum_{j=1}^k \beta_j f_j(\bar{x}) \quad (16)$$

$Z(\bar{x})$ is a Gaussian correlation function assumed to have mean zero and covariance

The $F(\beta, x)$ term is a "global" approximation for the entire design space based on a least squares fit to a set of data, while the $Z(\bar{x})$ term creates a "localized" correction based on it.

The covariance matrix of $Z(\bar{x})$ is expressed as:

$$Cov(Z(x^{(i)}), Z(x^{(j)})) = \sigma^2 \Re[R(x^{(i)}, x^{(j)})] \quad (17)$$

Where \Re is the correlation matrix and R is the correlation function and selected as:

$$R(x^{(i)}, x^{(j)}) = \exp\left\{-\theta_k \sum_{k=1}^n |x_k^{(i)} - x_k^{(j)}|^2\right\} \quad (18)$$

Where θ_k is the vector of unknown correlation parameter.

The concept of Mean Squared Error (MSE) is introduced to represent the distinction between $\hat{y}(\bar{x})$ and $y(\bar{x})$,

If MSE is minimized, $\hat{y}(\bar{x})$ becomes

$$\hat{y}(\bar{x}) = f^T \beta^* + r(x)^T R^{-1} (R - F \beta^*) \quad (19)$$

Where β^* is the obtained least squares fit:

$$\hat{\beta} = (f^T R^{-1} f)^{-1} R^{-1} y \quad (20)$$

$$\sigma^2 = \frac{(y - \hat{\beta} f)^T R^{-1} (y - \hat{\beta} f)}{n} \quad (21)$$

And $r(x)$ is the correlation vector between the response at a location x and the $x^{(1)}, x^{(2)}, \dots, x^{(n)}$ response values. The correlation vector is expressed as

$$r(x) = \{R(x, x^{(1)}), R(x, x^{(2)}), \dots, R(x, x^{(n)})\} \quad (22)$$

It is noted that both of prediction model variables implicitly depend on the parameter θ_k , and the maximum likelihood

estimation of θ_k can be obtained from solving the optimization problem below:

$$\max \left\{ -1/2 (n \ln \sigma^2 + \ln |R|) \right\}, \text{ subject to } 0 \leq \theta \leq \infty \quad (23)$$

As mentioned above, the constructing of kriging model can be thought as an N-dimensional optimization problem (N is the number of variables). If the correlation parameters are determined by the conventional numerical optimization methods, the optimal results is often dependent on the starting points for the solution searching, especially for the high-dimension problems, searching of the best θ_k would be very difficult.

In the present study, the modified CCGA is also used to search the best θ_k from the optimization problem defined by

equation (23). When the optimized θ_k is justified, the kriging model is completely defined and $\hat{y}(\bar{x})$ can be then predicted.

Once a sample is added, a new θ_k will be searched by CCGA, and kriging model will be then reconstructed (or updated).

5.5 Design of Experiment (DOE)

In the initialization of the kriging model, an appropriate design of experiment must be used to reduce the number of experiments and also produce a uniform distribution of samples. For a high-dimension problem, the construction of computer experiments is of crucial importance. Some frequently-used DOEs are compared in reference [19], and the Uniform Design Experimentation (UDE) are of better performance for the high-dimension problems, and it can help to achieve the above goal, thus chosen in the present study.

The number of samples is another key factor for the prediction ability of kriging model. For comparison, different set of points (50, 100, 150 and 300) are sampled respectively using (the Uniform Design Experimentation) for the 12-dimension ‘‘BUMP’’ problem. Then a group of kriging models are created and 10,000 random points are used to test all the kriging models. The mean and maximum error is shown in table 2.

Table 2 Comparison of different number of samples

Number of samples	Mean relative error	Max relative error
50	6.72%	9.45%
100	1.87%	3.39%
150	0.93%	2.56%
300	0.85%	2.37%

As shown in table 3, it is clear that the larger experimental sample points may produce a better performance for the approximate models for this specific DOE. However, for a highly nonlinear problem, adding one single sample point may only improve the local predictive accuracy of the kriging models in its close vicinity.

Clearly, unreasonable increase of experimental points may only increase the number of costly CFD simulation calling rather than the predictive accuracy. For the complicated problems, such as turbomachinery optimization, the number of experiments that can be achieved is often limited by the time-consuming CFD, which somehow constrains the predictive capacity even for the most robust approximate models and methods. Thus, the setting-up of DOE requires some careful considerations.

In the present study, in consideration of both the prediction precision of the model and available computational resources, an initial rough model is established at the first step, and it is improved gradually under the control of CCGA, which is detailed in section 5.5. The minimum samples for the 12-dimension quadratic regression analysis (as a part of kriging model) is $12 \times 13 / 2 = 98$, it is better to choose the number of experiments 20% larger than the minimum one, thus 120 CFD experiments are arranged to create the initial kriging model.

5.6 Automatically Updated Kriging Model Driven By CCGA

When the initialization of kriging model is completed, it will be used to replace the true objective function (i.e. the time-costly CFD simulation). Then the CCGA will be started to search in the design space. Once a potential superior individual is found on the basis of statistics, a decision will be made by the in-house code on whether or not it needs a updating. If is required, the true objective function evaluation will be conducted, and the obtained value is termed ‘true fitness’ and saved in the database to update the kriging model.

The CCGA combined with automatically updated kriging model is tested by the ‘‘BUMP’’ problems of $N=2, 6$ and 12 respectively. Fig.10 shows the plot for the 2-D bump problem (only 2-D problem can be visualized by picture) optimization results based on the automatically updated kriging model, and the obtained maximum objective function is 10000.0; which agree well with the analytical optimal solutions, as shown in Fig.9. The developed optimization method is justified.

Fig.12 shows the plot (curve surface) obtained using the automatically updated Kriging model for 2-D bump problem, where the black points distributed on the surface represent the samples for creating kriging models (43 in total). It is evidently that the black points are scattered over the entire 2-D space, but there is an intensive concentration in close neighborhood of the two biggest peaks, and this exactly illustrates the automatically updated Kriging model driven by the modified CCGA works very well, where the scattered points of the entire space representing the samples for initializing the Kriging model by means of the uniform design experimentation as described in section 5.4; and the concentrated points near two biggest peaks are automatically updated samples driven the CCGA according to potential superior individual performance.

As also shown from the comparison of Fig.12 and Fig.10, the kriging approximation is not accurate in the entire space of variables. But around biggest peaks, more samples are selected by the improved CCGA and evaluated by the real model of bump problem, and then used to update the kriging model, in such a way, the approximated model approaches very efficiently to the top peaks, and the CCGA can complete its searching with a limited number of real evaluations of objective function.

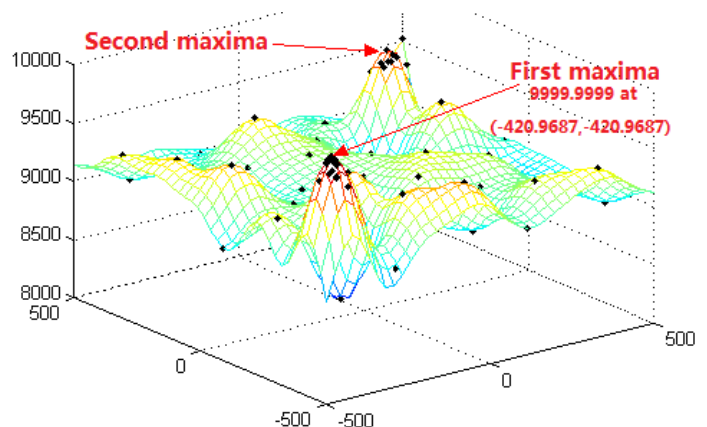


Fig. 12 Plot obtained using the automatically updated kriging model for 2-D bump problem

6 RESULTS AND DISCUSSION

The developed optimization framework is used to optimize the liquid turbine at design flow, some performance gain are obtained, which demonstrates the effectiveness of the developed optimization method.

With 200 generations and in total 212 callings of CFD prediction (120 CFD callings are necessary for initializing the kriging model. The 200 generations of CCGA evolutions, and 92 callings of CFD for nozzle and impeller geometry changes were decided by the CCGA algorithm), the CCGA has converged at the minimum of objective function value 0.549656 and the optimized solution to the liquid turbine obtained. Figure 13 presents the convergence history of the objective function. Variations of the nozzle vane and impeller geometry and overall performance for the optimized liquid turbine are analyzed and presented below.

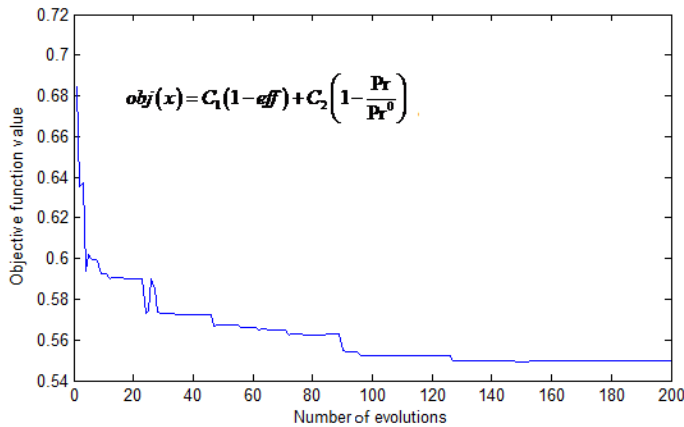


Fig. 13 Converged history of turbine optimization

The Figure 14 compares the optimized nozzle vane geometry with the original, and variation of the leading edge is evident.

For the optimal turbine stage, there is only 0.05° variation in stagger angle, the optimized stagger angle is very close to the original setting, the reason is that the initial stagger angle, 35° , used in the present optimization comes from our previously reported work [5], which conducted mainly for the stagger vane optimization, the initial nozzle vane setting used in the present turbine stage optimization is the previously optimized results. Some simplifications are used in our previous work, for example, the volute has not been included in the physical model used in [5], thus the optimized results of stagger angle are different from the present study, but the deviation is very small.

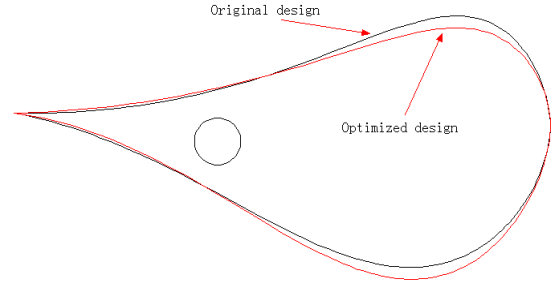


Fig. 14 Comparison of optimized turbine nozzle vane with the original one

Variation in the optimized impeller shape can be described by the variations of the impeller design variables. Table 3 presents the optimized impeller design variables together with that for the original impeller geometry, as shown in the figure, deviations in each of the six impeller design variables are evident after the optimizations.

Table 3 variable of impeller geometry changes

	Original	Optimized	Changes
α_1	0	0.571429	0.571429
α_3	0	-1.445378	-1.445378
β_{B0}^0	33	33.218487	0.218487
φ_R	3	3.170866	0.170866
φ_Z	3	3.142857	0.142857

With the mentioned modifications in both nozzle vane and impeller geometry, some overall performance gains have been produced by the optimized turbine. Table 3 presents the optimized turbine performance data together with the original ones. For the optimized turbine, improvement in the isentropic efficiency, expansion ratio and power output are visible, and somewhat decrease in both outlet temperature and absolute velocity can be seen simultaneously. The decrease in both outlet temperature and absolute velocity can somehow indicates less mechanical energy is wasted in the turbine stage, and it works more efficiently and outputs larger shaft power, which exactly supports the optimized performance data of overall turbine efficiency, power output and expansions, as shown in table 4.

Table 4 Optimized turbine performance at design flow

	Original	Optimized	Increase
Isentropic efficiency	84.83%	86.14%	1.54%
Expansion ratio	12.528	14.533	16.0%
Power output	187.93kw	190.21	1.23%
Temperature outlet	95.0816k	95.003k	-0.0786k
Absolute velocity outlet	25.212m/s	24.923m/s	-0.197m/s

As well known, turbine performance gains are directly due to an improvement in turbine flow behavior with the optimized geometry shape. Figure 15 presents the streamline at 50% span for both the original and optimized turbine geometry, it is visible that there is somewhat improvement in streamline distribution

near the blade surface for the optimized turbine, but other evident changes are not seen.

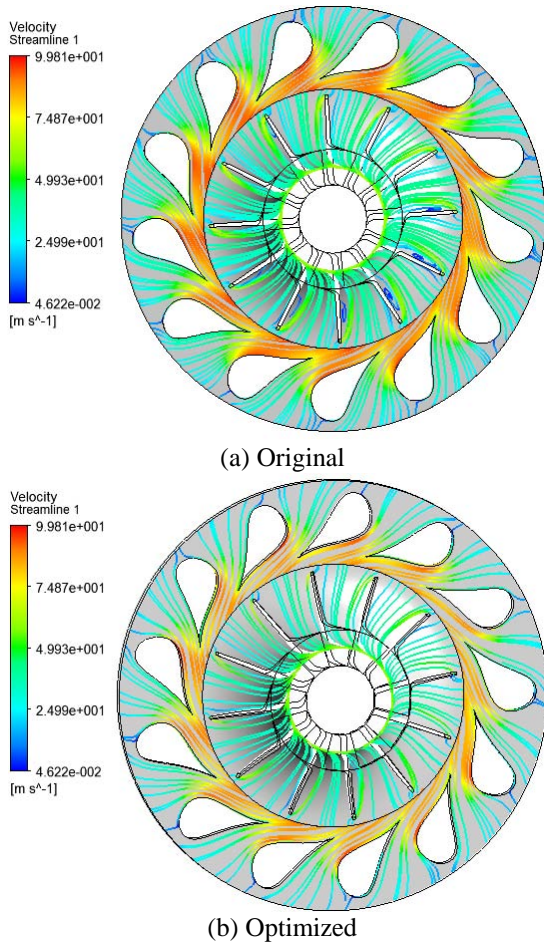


Fig. 15 Streamlines of turbine (50% span)

This is the initial study of our improved optimization framework using CFD. It is demonstrated that the optimal design method can help to reduce significantly the searching time for the optimal geometry design and improve the design solution to the liquid turbine. A small performance gain is obtained by optimization, but evident changes are hardly seen in the flow field data, for example figure 15.

As mentioned above, this is the initial step in applications of the developed optimization framework, performance gain of the optimized turbine is visible, but it is not as large as expected. The following are the main causes for this, which are also our major concerns in the near-future study:

Parameterization methods used in the present study for both nozzle vane and impeller blade are very preliminary, which much possibly have compromised the optimal performance gain. The 2-dimension nozzle is parameterized using two cubic B-spline curves, coordinates of the leading and trailing edges are fixed and ordinates for all the remaining vertex points are also held unchanged. In the present study, thus only 6 variables are used to represent the nozzle blade shape, which, the authors thought, may largely restrain the optimal searching space. On the other hand, impeller shape parameterization is

based on the analytical method, and the blade is described by an elliptic-curve equation. Such kind methods use a few variables to represent the geometry shape, and variations of the shape are severely limited, which can also restrain the optimal impeller geometry searching. Clearly robust parameterization methods are expected for both nozzle vane and impeller to obtain some substantial performance gains from turbine geometry optimization.

The prescribed bounds of optimization variables are also crucial influential factors on the optimal solutions, which define the variation range for each geometry parameterization variable and subsequently the optimal searching space. In the present study, in consideration of the convergence speed of the optimal solution and available computing resources, quite small variation ranges are prescribed for each geometry variable, we thought that this can obviously compromise the optimized solution. In the near-future study, in-depth investigation on setting up of optimization variable bounds will be conducted, which is expected to permit more optimized performance gains.

7 CONCLUSIONS AND FUTURE WORK

An optimization design method is developed, which is motivated by the optimal design of a cryogenic liquid turbine, based on which, an optimization framework is established through the combination of the in-house codes and commercial CFD software. It is validated through the optimization of the well-known bump problem. The liquid turbine is then optimized by this optimization frame and some performance gains are obtained. From the present investigation, the following conclusions have arisen

- The optimized impeller geometry, and nozzle vane geometry and stagger angle permits visible performance gain in both overall turbine efficiency and output power, which is due some improvement in flow behavior, where loss in the turbine is reduced and a somewhat temperature drop at turbine outlet is produce.
- The optimization framework has produced very quick optimal solutions for the turbine stage, which demonstrates the effectiveness of the optimization framework in dealing with the complex problem.

Future Work

Future work will be conducted in several aspects:

- Efficient geometry parameterization methods of less variables and high flexibility will be developed for both nozzle and impeller blade shape representation.
- Definition of the design space: small variation ranges of design variable can compromise the optimization gains, but large variation range can possibly lead to mal CFD simulation results and increase the optimal searching time as well. Thus, many factors must be taken into account in defining the design space. A good compromise is required, and this is left for future consideration.
- Some robust algorithm will be investigated and incorporated with the optimization framework, to improve further its convergence speed, globality, and solutions.

ACKNOWLEDGMENTS

The work is supported by the National 863 Plan of the Ministry of Science and Technology (Project No. 2007AA05Z202) and the National Natural Science Foundation of China under Grant 51006078(2010), and both are highly acknowledged by the authors.

NOMENCLATURE

About "Parameterization of impeller"

α_1	The angle between the external end-face of inducer and radial direction;
α_3	The angle between the internal end-face of inducer and radial direction;
β_{B0}^0	The blade angle in the average-radial of external end-face of inducer;
φ_R	The angle between pressure surface and suction surface of the impeller blade in the radial direction;
φ_Z	The angle between pressure surface and suction surface of the impeller blade in the axial direction;

About "Variable classification algorithm"

φ_Z	The number of variables
N_i	The population size of GA
$X_i(t)$	An individual of GA in t generation
$x_{ij}(t)$	Component of an individual (One of Variables)
$\bar{X}_{*i}(t)$	Mean Value of a variable in a population
$\sigma(x_{*i}(t))$	Variance of a variable in a population
$\rho(x_i, x_j)$	The relevance of two variables x_i and x_j

About "Improvements of CCGA"

f	The objective function value of one individual
P_c, P_m	Crossover rate and Mutation rate
Δ	Variation (Mutation)
r	Random numeral
T, t	Maximum generation and current generation

Superscript

$child, parent$	The parent generation and child generation
$*, '$	The transformational value

Subscript

max, min, avg	The maximum, minimum and average
-----------------	----------------------------------

About "Kriging model"

\hat{y}	Prediction value
\bar{x}	The vector variables
F	Regression model
β	Parameter of regression model

$Z(\bar{x})$	Correction model
Cov	Covariance matrix
R	Correlation function
θ_k	The vector of unknown correlation parameter;
$r(x)$	The correlation vector between x and the $x^{(1)}, x^{(2)}, \dots, x^{(n)}$;

REFERENCES

- [1] Johnson, L L., Renaudin, Gerard., 1996, "Liquid turbines improve LNG operations," Oil & Gas Journal, 94, pp. 31-36.
- [2] H Kimmel., 1997, "Speed controlled turbines for power recovery in cryogenic and chemical processing," World Pumps, 369, pp. 46-49.
- [3] Sun Quanhai, 2004, "Influence of liquid turbo-expander on an air-separation process performance," Cryogenic Technology, No.3., pp. 17-19.
- [4] Johnson, L.L.et al., 1995, "Improvement of natural gas liquefaction processes by using liquid Turbines," Conf.proc.Int. Conf.Exhib., Liquefied Nature Gas , pp. 1-11.
- [5] Wei Zhao, Jinju Sun, Hezhao Zhu, Cheng Li, Guocheng Cai, and Guohong Ma, 2008, "Numerical investigation of a cryogenic liquid turbine performance and flow behavior," ASME Paper No. GT2008-50391.
- [6] Yan REN, Jinju SUN, Rongye ZHENG, Peng SONG, and Ke WANG,2010, "Investigation of impeller strength for a cryogenic liquid turbine, " ASME Paper No. GT2010-23125.
- [7] Michalewicz, Zbigniew. Genetic Algorithms + Data Structures = Evolution Programs[M].Springer, 1992.
- [8] K. Deb and R. B. Agrawal. Simulated binary crossover for continuous search space. Complex Systems, 9(2):115--148, 1995.
- [9] Steck J, Rokhsaz K. Some applications for artificial neural networks in modeling of nonlinear aerodynamics and flight mechanics. AIAA Paper 97-0338, Reno, NV, January,1997.
- [10] Shyy W, Papila N, Vaidyanathan R, Tucker K. Global design optimization for aerodynamics and rocket propulsion components. Prog Aerospace Sci 2001;37:59--118.
- [11] Ratle A. Optimal sampling strategies for learning a fitness model. Proceedings of the 1999 Congress on Evolutionary Computation (CEC99). Washington, DC, USA, July,1999.
- [12] El-Beltagy M, Nair P, Keane A. Metamodeling techniques for evolutionary optimization of computationally expensive problems: promises and limitations. In: Banshaf W,et al. editors. Proceedings of GECCO99, Orlando, 1999.
- [13] ANSYS 12.1 HELP MANUAL
- [14] Potter, M.A., DeJong, K.A.: Cooperative coevolution: an architecture for evolving coadapted subcomponents. Evolutionary Computation 8(1), 1--29 (2000)
- [15] J.H. Holland, Adaptation in Natural and Artificial Systems, University of Michigan Press, Ann Arbor, 1975.
- [16] Xiaoyan Sun, Dunwei Gong, Xueyan Du. On linkage identification based coevolutionary population decomposition algorithm.CONTROL AND DECISION, 20(6), 2005.

- [17] Giunta Anthony A and Watson Layne T. A comparison of approximation modeling techniques: polynomial versus interpolating models [R] . AIAA 1998-4758.
- [18] E. Siah, T. Ozdemir, J. Volakis, P. Papalambros, and R. Wiese, Fast parameter optimization using kriging metamodeling [antenna em modeling/simulation], in Antennas and Propagation Society International Symposium, 2003. IEEE, vol. 2, 22-27 June 2003, pp. 76–79vol.2.
- [19] Kai-Tai Fang, Runze Li, Uniform design for computer experiments and its optimal properties, International Journal of Materials and Product Technology 2006 - Vol. 25, No.1/2/3 pp. 198 - 210